



Mesenchymal Stem Cell Transplantation Improves Regional Cardiac Remodeling Following Ovine Infarction

YUNSHAN ZHAO,^{a*} TIELUO LI,^{a*} XUFENG WEI,^a GIACOMO BIANCHI,^a JINGPING HU,^a
PABLO G. SANCHEZ,^a KAI XU,^b PEI ZHANG,^a MARK F. PITTENGER,^a ZHONGJUN J. WU,^a
BARTLEY P. GRIFFITH^a

Key Words. Adult stem cells • Mesenchymal stem cells • Stem cell transplantation • Myocardial infarction • Heart remodeling

ABSTRACT

Progressive cardiac remodeling, including the myopathic process in the adjacent zone following myocardial infarction (MI), contributes greatly to the development of cardiac failure. Cardiomyoplasty using bone marrow-derived mesenchymal stem cells (MSCs) has been demonstrated to protect cardiomyocytes and/or repair damaged myocardium, leading to improved cardiac performance, but the therapeutic effects on cardiac remodeling are still under investigation. Here, we tested the hypothesis that MSCs could improve the pathological remodeling of the adjacent myocardium abutting the infarct. Allogeneic ovine MSCs were transplanted into the adjacent zone by intracardiac injection 4 hours after infarction. Results showed that remodeling and contractile strain alteration were reduced in the adjacent zone of the MSC-treated group. Cardiomyocyte hypertrophy was significantly attenuated with the normalization of the hypertrophy-related signaling proteins phosphatidylinositol 3-kinase α (PI3K α), PI3K γ , extracellular signal-regulated kinase (ERK), and phosphorylated ERK (p-ERK) in the adjacent zone of the MSC-treated group versus the MI-alone group. Moreover, the imbalance of the calcium-handling proteins sarcoplasmic reticulum Ca^{2+} adenosine triphosphatase (SERCA2a), phospholamban (PLB), and sodium/calcium exchanger type 1 (NCX-1) induced by MI was prevented by MSC transplantation, and more strikingly, the activity of SERCA2a and uptake of calcium were improved. In addition, the upregulation of the proapoptotic protein Bcl-xL/Bcl-2-associated death promoter (BAD) was normalized, as was phospho-Akt expression; there was less fibrosis, as revealed by staining for collagen; and the apoptosis of cardiomyocytes was significantly inhibited in the adjacent zone by MSC transplantation. Collectively, these data demonstrate that MSC implantation improved the remodeling in the region adjacent to the infarct after cardiac infarction in the ovine infarction model. *STEM CELLS TRANSLATIONAL MEDICINE 2012;1:000–000*

INTRODUCTION

Interventional therapy to address the damage to the myocardium caused by myocardial infarction (MI) and cardiomyocyte death, inflammation, alterations of collagen matrix, microvascular rarefaction, structural and molecular remodeling, and the resultant functional impairment is a major challenge in cardiovascular medicine [1, 2]. Stem cell therapy is under study as a treatment option and potentially provides the necessary signals and factors for cellular repair to protect the damaged myocardium, and cellular repair to restore or regenerate the injured myocardium [3]. Among the varieties of stem cells described, bone marrow-derived mesenchymal stem cells (MSCs) are a leading therapeutic candidate because of their relative ease of isolation, stable

phenotype, and limited rejection [4, 5]. Several aspects of heart tissue regeneration, including increased blood vessel density, sparing of at-risk myocardium, and even new cardiomyocytes from MSC stimulation of cardiac stem cells, have been reported [6–10]. Accumulating evidence also suggests that MSCs provide benefits beyond their cell replacement potential by providing growth factors and cytokines and limiting inflammation [6]. The potential of MSC transplantation for the treatment of MI has been investigated in different animal models as well as in patients, and significant improvement of overall cardiac performance or local cardiac function has been reported [11–13]. In recent years, studies of the effects of MSC transplantation on structural and molecular tissue remodeling, which is a determinant of the clinical course of cardiac failure, have

^aArtificial Organ Laboratory, Department of Surgery, and ^bDepartment of Surgery, University of Maryland School of Medicine, Baltimore, Maryland, USA

*Contributed equally as first authors.

Correspondence: Zhongjun J. Wu, Ph.D., Artificial Organ Laboratory, University of Maryland School of Medicine, 10 South Pine Street, Room 443, Baltimore, Maryland 21201-1116, USA. Telephone: 410-706-7715; Fax: 410-706-0311; e-mail: zwu@smail.umaryland.edu; or Bartley P. Griffith, M.D., Department of Surgery, University of Maryland Baltimore, N4W94, 22 South Greene Street, Baltimore, Maryland 21201-1116, USA. Telephone: 410-328-3822; Fax: 410-328-2750; e-mail: bgriffith@smail.umaryland.edu

Received March 13, 2012; accepted for publication July 13, 2012; first published online in *SCTM EXPRESS* September 7, 2012.

©AlphaMed Press
1066-5099/2012/\$20.00/0

<http://dx.doi.org/10.5966/sctm.2012-0027>

become more prominent. Several groups have documented the reduced ventricular cavity dilation, the prevention of infarct expansion, and the mitigation of fibrosis after MSC transplantation [14–17]. However, the effects of MSC transplantation on the remodeling of surviving myocardium remain to be investigated.

The adjacent, nonischemic myocardium abutting the infarct is at potential peril of chronic stress following MI. Because of its unique juxtaposition between the noncontractile infarct scar and the viable contractile myocardium, the adjacent myocardium is imposed with highly abnormal stress patterns. The altered stress not only decreases strain in the adjacent region in the direction of the infarct but also transfers strain into the areas of myocardium that lack the contractile elements necessary to generate compensatory strain; these areas thus undergo remodeling, including strain alteration, myocyte hypertrophy, and imbalance of calcium-handling protein with increased apoptosis soon after MI [18–22]. This myopathic process in normally perfused myocardium appears to be localized initially to the myocardium abutting the infarct, but it later extends during the remodeling process to continuous segments, making these hypocontractile as well [23]. The remodeling in this adjacent area has been proposed as the main mechanism of the nonischemic infarct extension following MI, which plays an important role in promoting progressive cardiac remodeling and eventually cardiac failure [24, 25]. Therefore, the regional, nonischemic remodeling plays a key role in the development of progressive cardiac remodeling and eventually cardiac failure. However, thus far, little is known about the impact of MSCs on cellular and molecular remodeling in this region. We therefore used an ovine model of 25% chronic myocardial infarction by permanent ligation of the left anterior descending coronary artery and associated vessels to evaluate the impact of early intervention with local intracardiac injection of MSCs in the adjacent zone after cardiac infarction, and we examined the regional remodeling at the tissue, cellular, and molecular levels. Our results provide an important view into associated changes in the tissue abutting the infarct following MSC transplantation that may account for much of the improvement to adverse remodeling after myocardial infarction.

MATERIALS AND METHODS

Isolation and Culture of Ovine MSCs

Fresh bone marrow aspirates for preparation of allogeneic MSCs were obtained from the iliac crest of adult sheep (approximately 1–4 years old) under general anesthesia according to procedures approved by the animal care and use committee of the University of Maryland School of Medicine. After dilution with the same volume of 0.9% saline solution, the bone marrow aspirates were layered on Ficoll-Paque Premium (1.077 g/ml; GE Healthcare, Uppsala, Sweden, <http://www.gehealthcare.com>) and centrifuged for 40 minutes at 1,600 rpm at room temperature. The visible middle layer containing enriched bone marrow mononuclear cells (MNCs) was collected and washed with three volumes of phosphate-buffered saline (PBS), and the cells were centrifuged to remove any remaining Ficoll solution. Isolated bone marrow MNCs were resuspended and plated in Dulbecco's modified Eagle's medium (DMEM) (Gibco, Carlsbad, CA, <http://www.invitrogen.com>) with low glucose supplemented with penicillin (100 IU/ml)/streptomycin (100 µg/ml) and 10% (vol/vol)

MSC fetal bovine serum (FBS) (Gibco), incubated at 37°C in the presence of 5% CO₂. After 24 hours, the nonadherent cells were removed, and fresh complete medium was added. Medium was changed every 2 days by changing half of the volume with fresh complete medium. MSCs were subcultured using TrypLE Express (Gibco) when at 70%–80% confluence.

Flow Cytometric Analysis

Flow cytometric analysis was used to characterize the cell surface antigen expression of ovine MSCs using markers positively and negatively associated with MSCs. Cells were incubated with a primary antibody mouse anti-sheep CD44 (AbD Serotec, Raleigh, NC, <http://www.ab-direct.com>), mouse anti-human CD166 (BD Biosciences, San Diego, CA, <http://www.bdbiosciences.com>), mouse anti-human CD34 (BD Biosciences), mouse anti-sheep CD45 (AbD Serotec), mouse anti-human CD105 (BD Biosciences), mouse anti-human CD106 (BD Biosciences), or isotype-matched control (AbD Serotec) for 20 minutes at room temperature. After being washed to remove unbound primary antibody, cells were incubated for 20 minutes in a 1:100 dilution of Alexa Fluor 488-conjugated goat anti-mouse IgG on ice. Flow cytometric analysis was performed using a FACSCalibur analyzer (Becton, Dickinson and Company, Bohemio, NY, <http://www.bd.com>). Typically, for each sample 5,000 events were analyzed on the flow cytometer and stored as list mode data for further analysis using WinMDI software (Windows Multiple Document Interface Flow Cytometry Application; Joseph Trotter). Positive fluorescence was defined as the level of fluorescence greater than 99% of the corresponding isotype-matched control antibody.

Osteogenic, Chondrogenic, and Adipogenic Differentiation

To cause differentiation of MSCs toward osteoblasts, chondrocytes, and adipocytes, cells at passage 4 were seeded onto 12-well plates at 1×10^4 cells per cm² for adipogenesis and 5×10^3 cells per cm² for osteogenesis or at the center of multiwell plate wells with 5-µl droplets of cell solution of 1.6×10^7 for chondrogenesis in DMEM supplemented with penicillin (100 IU/ml)/streptomycin (100 µg/ml) and 10% (vol/vol) MSC FBS (Gibco), incubated at 37°C in the presence of 5% CO₂. Two days later, culture medium was replaced with differentiation medium (Gibco), and it was changed every 2 days thereafter. At 14 days for adipogenesis and 28 days for osteogenesis and chondrogenesis, samples were fixed with 4% paraformaldehyde for 30 minutes. Histological staining was performed using Oil Red O for adipocytes, Alcian blue for chondrocytes, and alizarin red for osteoblasts.

MI Protocol and Sonomicrometry Array Localization

An MI was surgically induced in 10 male sheep (5 MI only, 5 MI+MSC) using our published method [21]. In addition, four sheep were used as the sham group. For the sham group, sheep underwent the same surgical procedure without MI and MSC treatment. Briefly, adult sheep weighing 40–60 kg were anesthetized and instrumented. Polypropylene snares were placed around the left anterior descending and second diagonal coronary arteries and momentarily tightened (<30 seconds) to demarcate the border of the future infarct. Four specific transducers (2 mm; Sonometrics Corporation, London, ON, Canada,

<http://www.sonometrics.com>) were placed at the superior, inferior, medial, and lateral aspects of the transiently ischemic myocardium, and an additional transducer was placed in the center of this ischemic region. An additional 11 transducers were sutured into the mid-myocardium of the left ventricular (LV) free wall to create a final array of three short-axis aligned rows of five transducers with an additional transducer in the apex. The wires of the transducers were secured together with silk ties and tunneled subcutaneously, and their respective skin buttons were exposed to allow for future data acquisition. An anteroapical infarction was produced by ligating the left anterior descending artery and its diagonal branches, resulting in an infarction of approximately 25% of the LV mass. This technique has been shown to reproducibly create MI of consistent size. All animals were treated and cared for in accordance with the National Institutes of Health *Guide for the Care and Use of Laboratory Animals* (National Research Council, Washington, DC, 1996). The sheep were randomized to receive either nothing or a specific concentration of MSCs. For the purposes of control values for the subsequent myocardial biochemical analysis, LV myocardial samples were collected from the sham sheep. Areal strain (ϵ) between any pair of triangular crystals at two specific time frames can be calculated as follows:

$$\epsilon_{\text{con}} = \frac{S_{\text{ED}} - S_{\text{ES}}}{S_{\text{ED}}} \times 100\%, \epsilon_{\text{rem}} = \frac{S_{\text{ED}} - S_{\text{EDpreMI}}}{S_{\text{EDpreMI}}} \times 100\%$$

where S_{ED} and S_{ES} indicate the triangular area at end diastolic (ED) and end systolic (ES) instants, and S_{EDpreMI} is the triangular area at ED instant pre-MI. ϵ_{con} and ϵ_{rem} are the contractile strain and remodeling strains, respectively. The contractile strain, defined as LV deformation during an individual cardiac cycle, was used to assess regional myocardial contractility. The remodeling strain was defined as LV deformation over time and was calculated by comparing the end-diastole geometries at one data collection time point relative to the pre-MI measurement.

Preparation of MSCs for Injection

Allogeneic MSCs at passages 4–5 were harvested with TrypLE Express (Gibco) and resuspended in PBS. Four hours post-MI, a total of 2×10^8 cells in 0.3 ml were delivered by direct injection into the clearly identifiable border zone region adjacent to the infarct on the wall of the LV. A total of six injections were performed in each animal, with each injection containing $\sim 3.33 \times 10^7$ cells.

Histological Staining and Detection of Apoptosis by Terminal Deoxynucleotidyl Transferase dUTP Nick-End Labeling

Tissue samples of the remote and adjacent regions harvested at 12 weeks after MI were fixed, embedded in paraffin, and cut into 5- μm -thick sections. The sections were stained with hematoxylin and eosin, examined under a microscope (Axioskop; Carl Zeiss, Jena, Germany, <http://www.zeiss.com>), and digitally imaged. Cardiomyocyte size was calculated from the recorded digital images by using ImageJ software (NIH). For the detection of apoptosis, tissue sections were deparaffinized and permeabilized with proteinase K (25 $\mu\text{g}/\text{ml}$ in 100 mM Tris HCl). An in situ apoptotic cell death detection kit (TMR red; Roche Applied Science, Indianapolis, IN, <https://www.roche-applied-science.com>) based on the terminal deoxynucleotidyl transferase dUTP nick-end labeling (TUNEL) assay was used per the manufacturer's in-

structions to detect apoptotic cells. Sections were mounted with antifade Vectashield mounting medium containing 4',6-diamidino-2-phenylindole (DAPI) (Vector Laboratories, Burlingame, CA, <http://www.vectorlabs.com>) to stain DNA in the nuclei. Sections were examined with a Zeiss Axiovert 200 microscope and a Zeiss LSM 510 META laser scanning confocal microscope. Quantitative analysis of apoptotic nuclei was performed on two or three heart sections from four or five different hearts. The percentage of apoptotic nuclei per section was calculated by counting the total number of TUNEL staining nuclei divided by the total number of DAPI-positive nuclei in 10 randomly selected fields at a magnification of $\times 20$.

For picrosirius red staining, 5- μm paraffin sections were deparaffinized with standard xylene/ethanol series and rinsed with distilled water. The sections were immersed in 0.2% phosphomolybdic acid for 1 minute followed by staining in 0.1% Sirius red in saturated picric acid for 90 minutes. The slides were then washed with 0.01 N HCl for 2 minutes, rinsed with 70% ethanol followed by 100% ethanol and then xylene, and mounted using Permount (Fisher Scientific, Pittsburgh, PA, <http://www.fishersci.com>). The sections were examined under the Zeiss Axiovert 200 microscope (Carl Zeiss USA, Thornwood, NY, <http://www.zeiss.com/microscopy>).

Determination of SERCA2a Activity and ^{45}Ca Uptake

The ATPase assay and thapsigargin (Tg)-sensitive ^{45}Ca uptake were performed based on the method of Kyte [26] and Xu et al. [27] with some modifications. Briefly, cardiac muscle sarcoplasmic reticulum (SR) vesicles were isolated according to the method developed by Chu et al. [28] with modifications similar to those described previously [29]. Calcium-45 (^{45}Ca) at a concentration of 37.92 mCi/ml was from PerkinElmer Life and Analytical Sciences (Boston, MA, <http://www.perkinelmer.com>). Tg, a specific inhibitor of cardiac sarcoplasmic reticulum Ca^{2+} adenosine triphosphatase (SERCA2a), was from LC Laboratories (Woburn, MA, <http://www.lclabs.com>). The enzymatic activity was defined as the Tg-sensitive hydrolysis of ATP in the presence of Ca^{2+} (10 μM). The incubation mixture contained 15 mM imidazole/HCl, pH 7.4, 3 mM ATP, and 5 mM Mg^{2+} in a final volume of 0.5 ml and was brought to and maintained at 37°C in a water bath. The reaction was initiated by adding SR vesicles and stopped after 30 minutes. The color was allowed to develop for 30 minutes at room temperature, and the phosphate generated in the reaction was then determined spectrophotometrically at 700 nm. For the measurement of ^{45}Ca uptake, in addition to cardiac (0.15 mg/ml) SR vesicles, the reaction mixture contained Ca^{2+} (10 mM), ^{45}Ca (1 mCi/ml), Mg^{2+} (5 mM), and ATP (3 mM). Samples were incubated in the presence and absence of Tg at 37°C for 20 minutes. The reaction was terminated by centrifuging the sample at 14,000 rpm for 15 minutes, and the pellet was washed three times with 15 mM imidazole/HCl buffer, pH 7.2, and then dissolved in 100 ml of 10% SDS solution. The radioactivity was determined by a β -scintillation counter. Any ^{45}Ca transport in the presence of Tg was considered to represent non-specific ^{45}Ca uptake.

Western Blot Analysis

Immunoblotting was performed as described previously [21, 22]. In brief, tissue samples corresponding to different regions were collected, rapidly frozen in liquid nitrogen, and stored at -80°C .

Frozen tissue samples were homogenized in radioimmunoprecipitation assay buffer, separated by SDS-polyacrylamide gel electrophoresis, transferred to nitrocellulose polyvinylidene difluoride membrane, and probed with specific primary antibodies. Protein loading was controlled by probing for glyceraldehyde-3-phosphate dehydrogenase (GAPDH) (Santa Cruz Biotechnology Inc., Santa Cruz, CA, <http://www.scbt.com>). Expressions of phosphatidylinositol 3-kinase (PI3K α , PI3K γ) and extracellular signal-regulated kinases (ERK and phosphorylated [p-] ERK), SERCA2a (1:2,000 dilution; Novocastra Ltd., Newcastle upon Tyne, U.K., <http://www.novocastra.co.uk>), sodium/calcium exchanger type 1 (NCX-1) (1:500 dilution; Abcam, Cambridge, MA, <http://www.abcam.com>), and phospholamban (PLB) (1:2,000 dilution; Affinity BioReagents, Golden, CO, <http://www.pierce-antibodies.com>) were digitized and quantified with the UN-SCAN-IT gel TM 5.1 software (Silk Scientific, Orem, UT, <http://www.silkscientific.com>), which is sensitive to Western blot development by enhanced chemiluminescence (Amersham Biosciences, Piscataway, NJ, <http://www.amersham.com>). The densitometric result was expressed as the ratio of the target protein to GAPDH and normalized with that from the healthy heart tissue.

Statistical Analysis

All data are presented as mean \pm SEM. One-way repeated measures analysis of variance (ANOVA) was used to compare differences among groups. All ANOVAs were followed by multiple comparisons with the least significant difference correction. The significance level (p) was set at .05.

RESULTS

Characterization of MSCs

MSCs isolated by Ficoll gradient centrifuge and expanded as described above were characterized by flow cytometry, microscopy, and differentiation assay. The MSCs uniformly displayed a high level of expression of the hyaluronan receptor CD44 and CD166 and lacked expression of the leukocyte marker CD45 and the endothelial marker CD34 (Fig. 1A). Furthermore, the majority of antibodies reactive with human MSCs did not exhibit any reactivity with ovine MSCs, including CD106 and CD105 (Fig. 1A). Morphological observation showed that the MSCs exhibited spindle-shaped, fibroblastic morphology in culture (Fig. 1B). At passage 4, the MSCs readily differentiated into Oil Red O-positive adipocytes (Fig. 1C), alizarin red-positive mineralizing cells (osteocytes) (Fig. 1D) or Alcian blue-positive chondrocytes (Fig. 1E) when incubated in the respective differentiation media for 14 days of adipogenesis or 28 days of osteogenesis and chondrogenesis.

Reduction of Cardiac Strain Alteration by MSC Transplantation

Regional contractile and remodeling strains in the adjacent and remote zones of the MI and the MSC-treated groups were evaluated using sonomicrometry transducers implanted on the surface of the heart (Fig. 2A). MI induced the reduction in contractile function (from -15% to -10%) immediately after infarction in both the adjacent zone and remote zone (Fig. 2C). The contractility gradually recovered to the level of preinfarction in the remote zone of both the MI group and the MSC-treated group (Fig. 2C). However, the recovery of the contractility was observed in

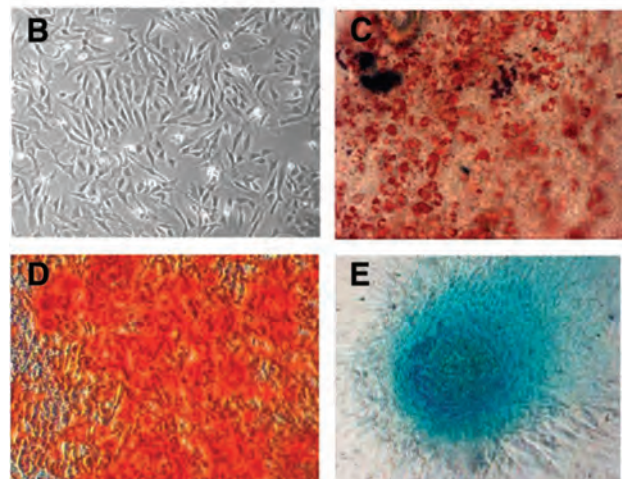
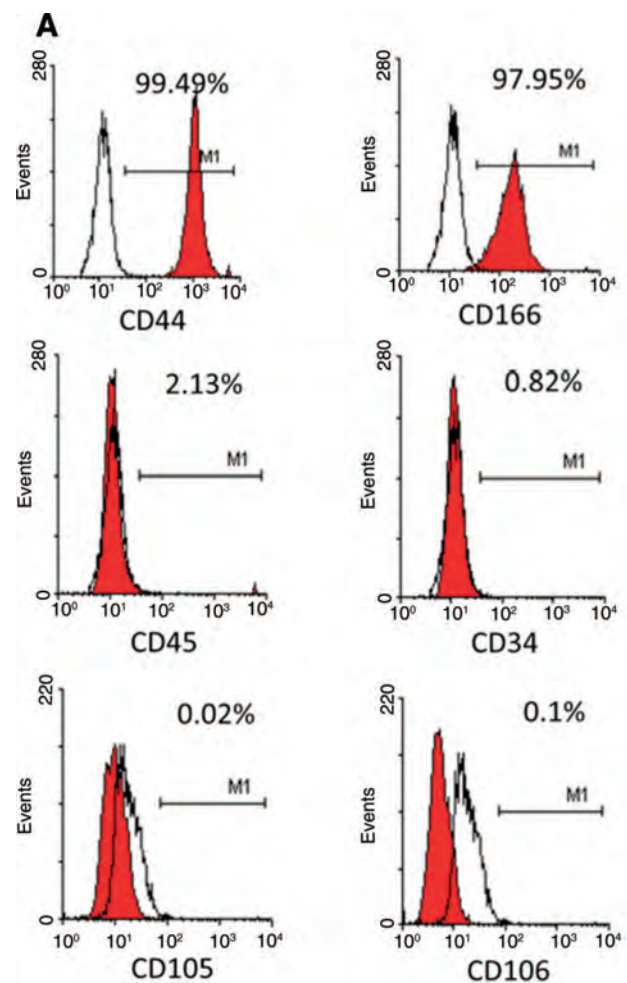


Figure 1. Characterization of ovine mesenchymal stem cells (MSCs). MSCs at passage 4 were analyzed by flow cytometry for cell surface markers and by microscopy for morphology, and differentiation assays were performed. **(A):** Flow cytometric analysis of cell surface markers of the MSCs, showing that the MSCs displayed a high level of expression of the hyaluronan receptor CD44 and ALCAM CD166, displayed reactivity to CD105 and CD106, and lacked expression of the leukocyte marker CD45 and the hematopoietic marker CD34 (M1, gate range). **(B–E):** Differentiation of the MSCs **(B)** showed positive staining toward adipocytes (Oil Red O) **(C)**, osteoblasts (alizarin red staining) **(D)**, and chondrocytes (Alcian blue) **(E)**.

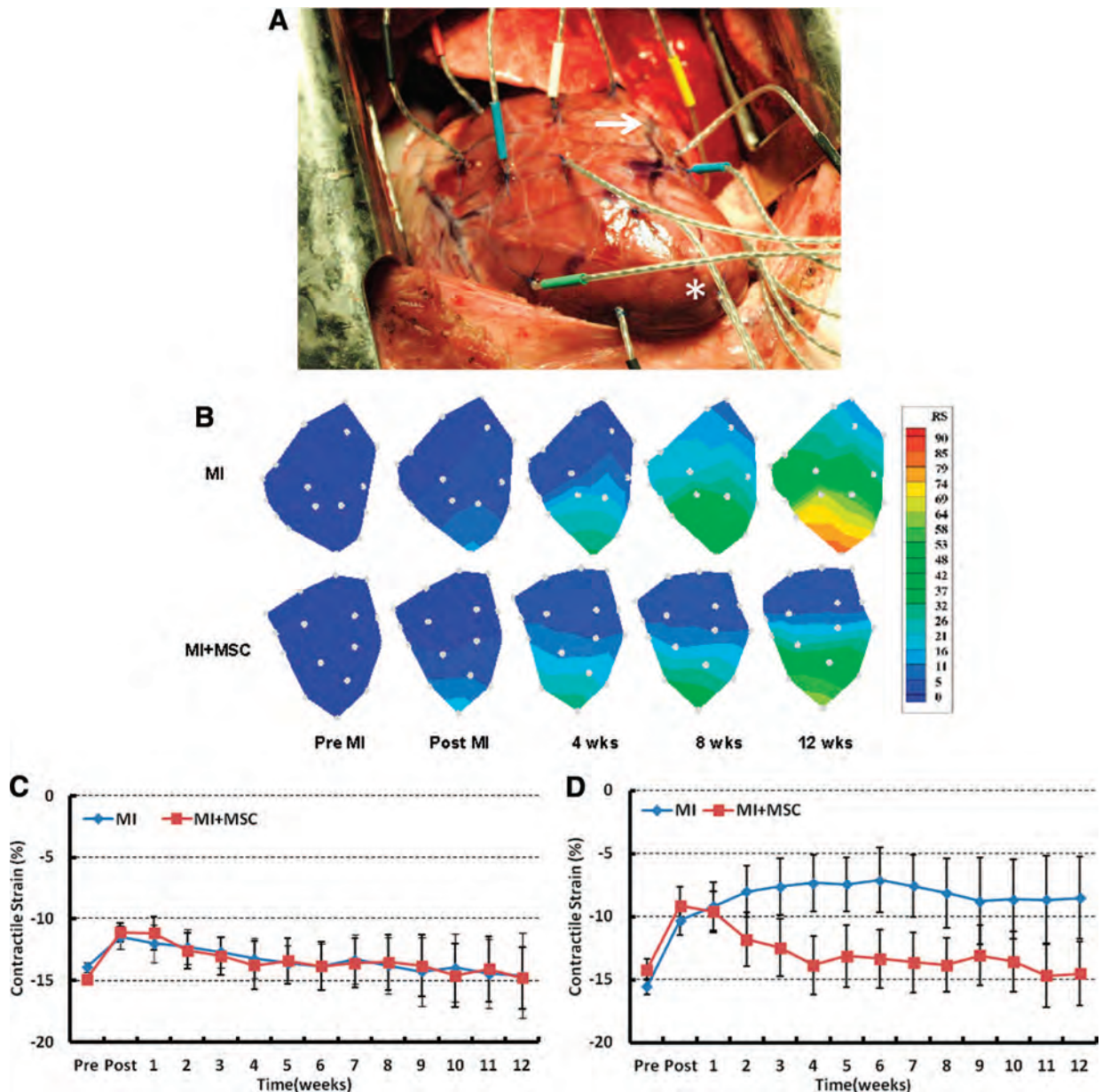


Figure 2. Effects of MSC transplantation on the remodeling and contractile strain in the adjacent and remote zones. **(A):** Photograph of the infarcted sheep heart on day 1 with the sonocrystals implanted. Solid arrow identifies initial left anterior descending ligation site. *, heart apex. **(B):** Alteration of cardiac strain was detected by the sonocrystals on the surface of the heart, showing the reduction in left ventricular remodeling strain (expansion) by MSC transplantation. **(C, D):** Alterations of contractile strain in the remote zone **(C)** and adjacent zone **(D)** showing the reduction of contractile strain alteration in the adjacent zone by MSC transplantation. Abbreviations: MI, myocardial infarction; MSC, mesenchymal stem cell.

the adjacent zone of the MSC-treated group and almost reached the level of preinfarction by 4 weeks, whereas the contractility in the adjacent zone of the MI group remained depressed (Fig. 2D).

Cardiac Hypertrophy Was Attenuated by MSC Implantation

To investigate the effects of MSC transplantation on hypertrophy, the cardiomyocyte size and the expression of hypertrophy-related signaling proteins were assessed in the adjacent and remote zones of the sham, MI, and MSC-treated groups. Examination of the cardiomyocyte cross-sectional area confirmed that the cardiomyocytes in the MSC-treated group had a

basal hypertrophy, a little larger than but not significantly different from sham group in the adjacent zone, whereas the ones in the MI group developed marked hypertrophy ($3,888.00 \pm 653.37$ vs. $2,533.00 \pm 144.37$; MI vs. sham, $p < .05$) in the adjacent zone by 12 weeks (Fig. 3A, 3B). There was a small increase in cardiomyocyte size in the remote zones of both the MI and the MSC-treated hearts compared with the sham group, but there was no significant difference among these three groups (Fig. 3A, 3B). Figure 3C shows representative photographs of picosirius red staining of heart sections of the sham, MI, and MSC-treated groups for collagen deposition after 12 weeks. Less collagen staining was found in the adjacent regions of animals that received MSCs.

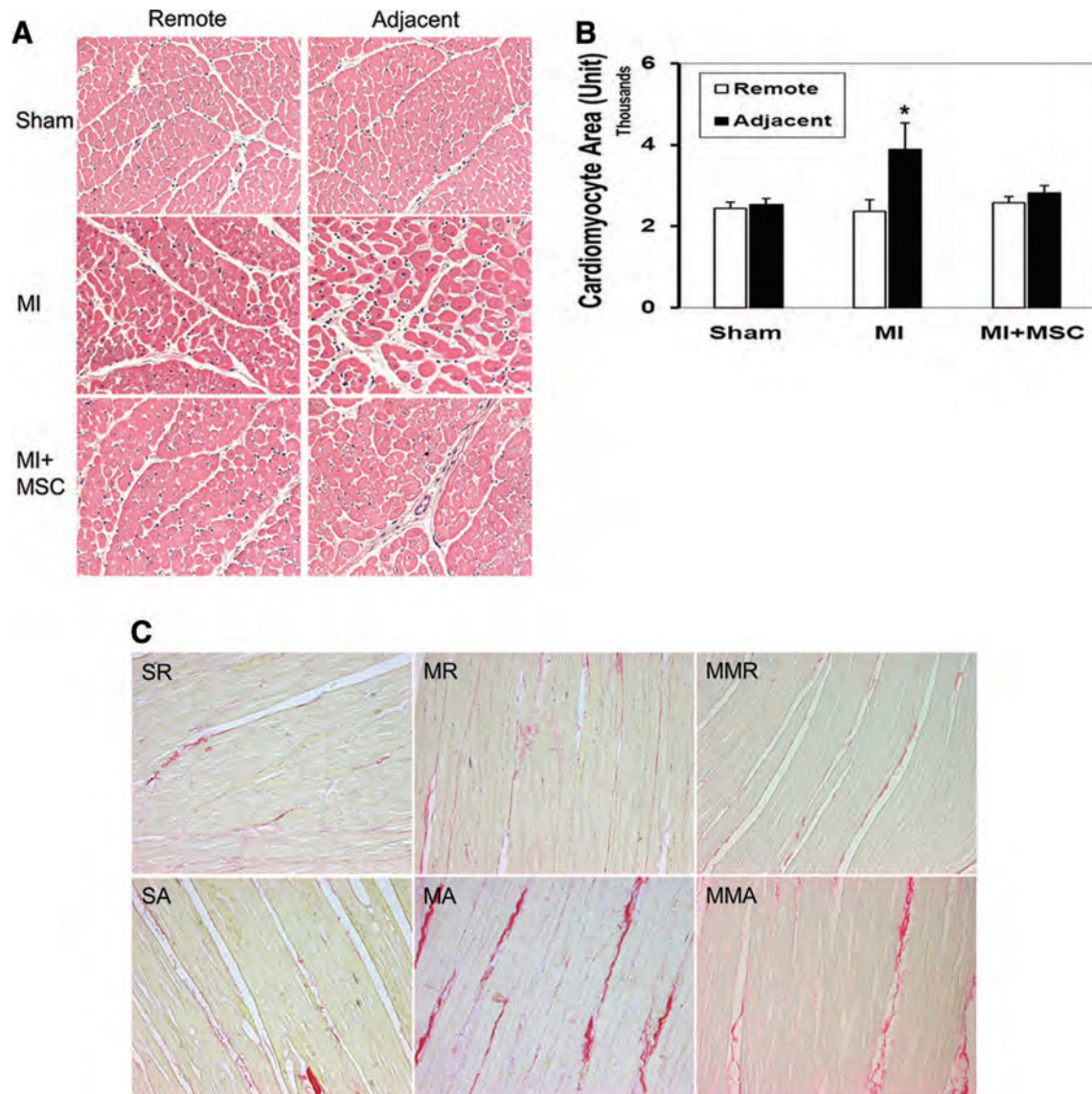


Figure 3. Attenuation of cardiomyocyte hypertrophy in the adjacent zone of the MSC-treated group. **(A):** Representative images of heart tissue cross-sections stained by hematoxylin and eosin in the adjacent and remote zones of the sham, MI, and MSC-treated groups. **(B):** Quantitative analysis of cardiomyocyte size shows that the hypertrophy of cardiomyocytes in the adjacent zone was significantly attenuated by MSC transplantation. *, $p < .05$ versus other groups. **(C):** Picrosirius red staining of heart sections for collagen deposition after 12 weeks. SR and SA represent two sections in sham animals that showed some staining. MR and MA are sections from the myocardial infarct, remote and adjacent; there was a clear increase in collagen staining in the adjacent region. MMR and MMA are sections from the remote and adjacent myocardial infarct regions in animals that received MSCs. Note that less collagen staining was found in the adjacent regions of animals that received MSCs. Abbreviations: MA, myocardial infarct adjacent; MI, myocardial infarction; MMA, MSC-treated myocardial infarct adjacent; MMR, MSC-treated myocardial infarct remote; MR, myocardial infarct remote; MSC, mesenchymal stem cell; SA, sham adjacent; SR, sham remote.

Accordingly, the expression of hypertrophy-related signal proteins PI3K α , PI3K γ , and p-ERK/ERK, which were significantly upregulated in the adjacent zone of the MI group (0.39 ± 0.05 , 0.41 ± 0.04 , 0.61 ± 0.10 , and 0.77 ± 0.18 , respectively; PI3K α , PI3K γ , and p-ERK/ERK 44 kDa, p-ERK/ERK 42 kDa) compared with the sham group (0.25 ± 0.03 , 0.24 ± 0.03 , 0.42 ± 0.04 , and 0.53 ± 0.05), was normalized in the same region of the MSC-treated group (0.28 ± 0.02 , 0.28 ± 0.03 , 0.42 ± 0.04 , and 0.58 ± 0.04), almost equaling the amount in the sham group (Fig. 4A–4E). No significantly altered expression of PI3K α , PI3K γ , and p-ERK/ERK was observed in the remote zone of sham, MI, and MSC-treated groups (Fig. 4A–4E).

MSC Implantation Normalized the Expression of Calcium-Handling Proteins

The calcium-handling proteins SERCA2a, PLB, and NCX-1 were assayed for expression level in the sham, MI-only, and MSC-treated groups by Western blot. Significant downregulation of SERCA2a (1.95 ± 0.16 vs. 1.53 ± 0.07 ; sham vs. MI, $p < .05$) and PLB (2.38 ± 0.22 vs. 1.45 ± 0.32 ; sham vs. MI, $p < .05$) and upregulation of NCX-1 (0.85 ± 0.09 vs. 1.23 ± 0.09 ; sham vs. MI, $p < .05$) were observed in the adjacent zone of the MI group compared with the sham group (Fig. 5A–5E). However, the imbalanced expression was completely normalized by MSC

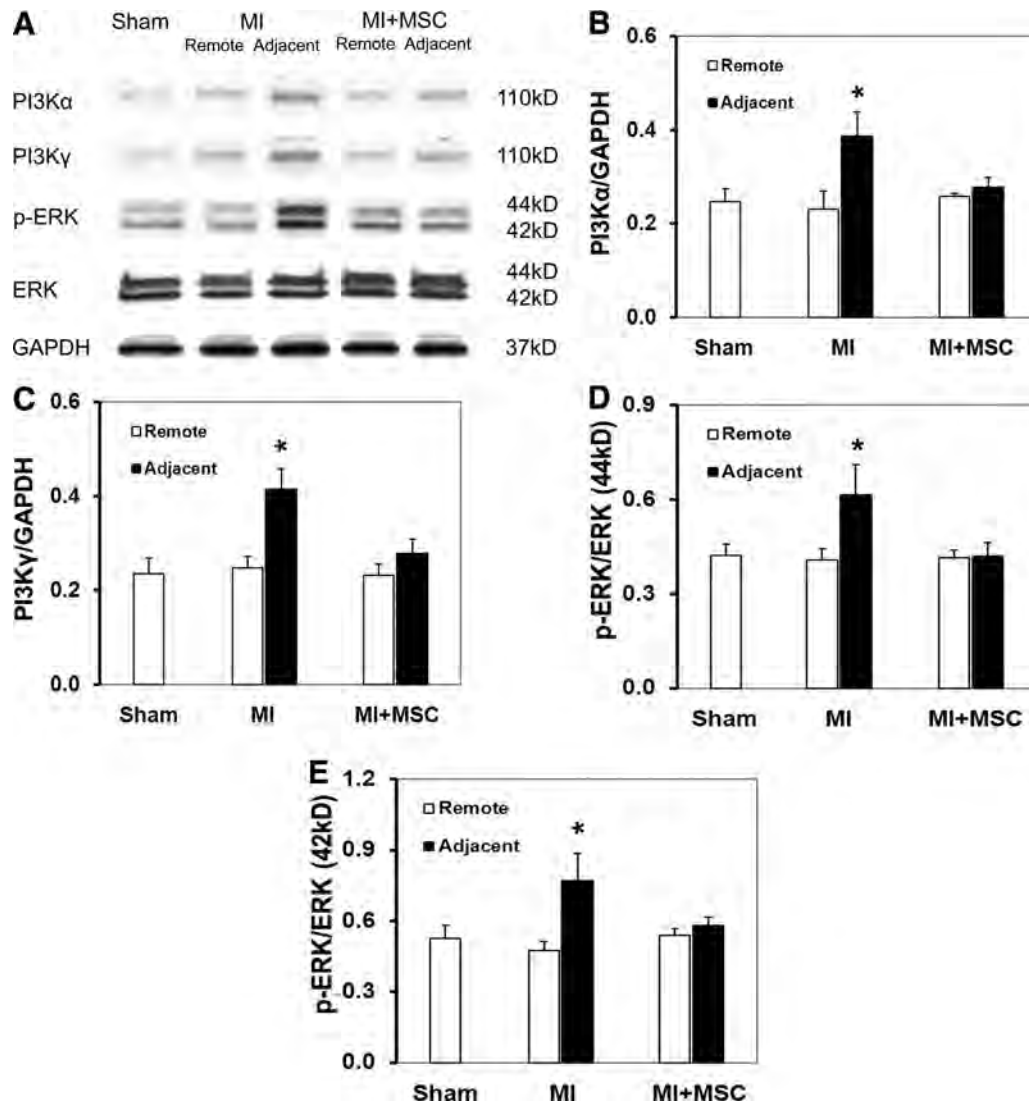


Figure 4. Expression of hypertrophy-related signaling proteins in the adjacent and remote zones of the MI and MI+MSC groups, as well as the sham group, at 12 weeks. **(A)**: Representative photomicrographs of Western blot, showing that the upregulation of PI3K α , PI3K γ , and p-ERK induced by myocardial infarction in the adjacent zone was normalized by MSC transplantation. **(B–E)**: Quantitative analysis of PI3K α **(B)**, PI3K γ **(C)**, and p-ERK **(D, E)** quantified and confirmed their normalization after MSC delivery on the infarct adjacent tissue. *, $p < .05$. Abbreviations: ERK, extracellular signal-regulated kinase; GAPDH, glyceraldehyde-3-phosphate dehydrogenase; MI, myocardial infarction; MSC, mesenchymal stem cell; p-ERK, phosphorylated extracellular signal-regulated kinase; PI3K, phosphatidylinositol 3-kinase.

transplantation (Fig. 5A–5E). There were no differences in expression of SERCA2a, PLB, and NCX-1 in the remote zones of the sham, MI, and MSC-treated groups (Fig. 5A–5E). More strikingly, the Ca²⁺ ATPase (SERCA2a) activity ($53 \pm 4\%$ vs. $184 \pm 55\%$, MI vs. MSC-treated) and the ⁴⁵Ca²⁺ uptake ($48 \pm 13\%$ vs. $191 \pm 27\%$, MI vs. MSC-treated) were significantly improved by MSC transplantation in the adjacent zone (Fig. 5F, 5G). No significant changes in Ca²⁺ ATPase activity or ⁴⁵Ca²⁺ uptake were observed in the remote zones of the sham, MI, and MSC-treated groups (Fig. 5F, 5G).

MSC Transplantation Inhibited Cardiac Apoptosis

To examine whether MSC transplantation inhibits the apoptosis of the regional myocardium in the adjacent zone, proteins of proapoptosis and apoptotic cardiomyocytes in the sham, MI, and MSC-treated groups were assayed by Western blotting and TUNEL staining, respectively. Significantly increased expression

of Bcl-xL/Bcl-2-associated death promoter (BAD) (0.82 ± 0.11 vs. 0.54 ± 0.03 ; MI vs. sham, $p < .05$) in the adjacent zone of the MI group has been observed compared with the sham group (Fig. 6A, 6B). However, the upregulation was completely normalized in the adjacent zone of the MSC-treated group (Fig. 6A, 6B). No significant change in the expression of BAD was observed in the remote zone of the sham, MI, and MSC-treated groups (Fig. 6A, 6B). TUNEL staining also showed that significant increase of apoptotic cells induced by MI in the adjacent zone was inhibited by MSC transplantation (5.9 ± 0.3 vs. 0.6 ± 0.1 ; MI vs. sham, $p < .05$). There was no difference in apoptotic cells in the remote zone of the sham, MI, and MSC-treated groups (Fig. 6C, 6D). We also examined the expression of Akt and phospho-Akt in the sham and infarcted animals, and this demonstrated a continued elevated expression of phospho-Akt in the MI animals that was not seen in the MI animals treated with MSC injection (Fig. 6E, 6F).

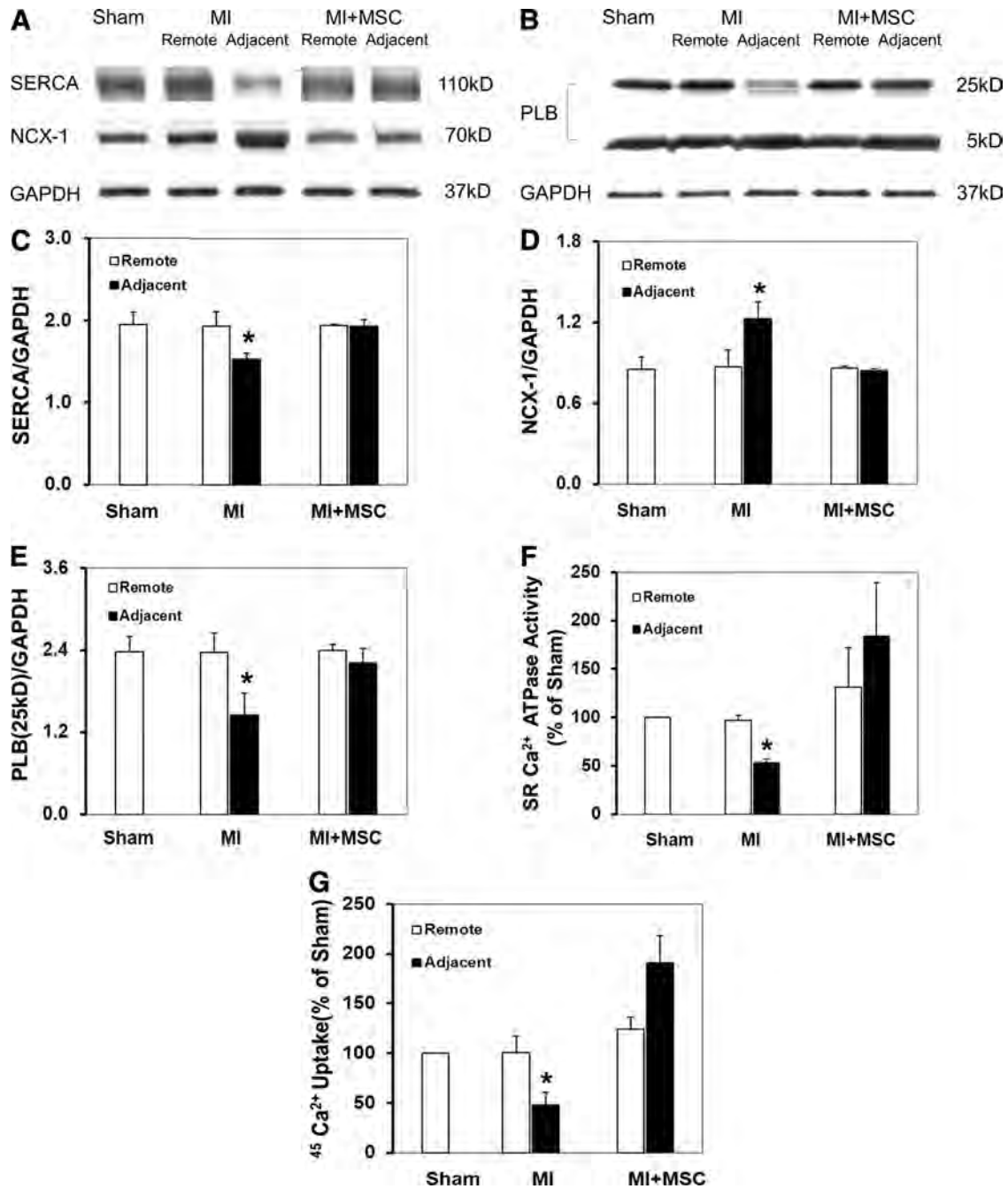


Figure 5. Expression and activity of calcium-handling proteins in the adjacent and remote zones of the MI and MI+MSC groups at 12 weeks. **(A, B):** Representative photomicrographs of Western blots, showing that the upregulation of NCX-1 and downregulation of SERCA2a and PLB induced by myocardial infarction in the adjacent zone was normalized by MSC transplantation. **(C–E):** Quantitative analysis of SERCA2a, NCX-1, and PLB expression demonstrated normalization due to MSC delivery. **(F, G):** Effects of MSC transplantation on cardiac SERCA2a function, showing that the SERCA2a activity **(F)** and ⁴⁵Ca²⁺ uptake **(G)** were improved by MSC transplantation. *, $p < .05$. Abbreviations: GAPDH, glyceraldehyde-3-phosphate dehydrogenase; MI, myocardial infarction; MSC, mesenchymal stem cell; NCX-1, sodium/calcium exchanger type 1; PLB, phospholamban; SERCA, sarcoplasmic reticulum Ca²⁺ adenosine triphosphatase (SERCA2a); SR, sarcoplasmic reticulum.

DISCUSSION

Here, we demonstrated that the myopathic process induced by MI in the adjacent zone was improved by MSC transplantation in a clinically translational ovine model, with cardiac remodeling strain improved, cardiac hypertrophy lessened, cardiac apoptosis reduced, and expression of calcium-handling proteins normalized. The results provide new evidence detailing the

therapeutic effects of MSC transplantation on progressive cardiac remodeling following MI. The timing of the injections was designed to model what might be possible clinically, in a 4-hour postinfarction window. The cells were delivered epicardially into the mid-myocardium, simulating an open chest procedure, but delivery is likely possible with cardiac transventricular delivery in the interventional catheterization laboratory.

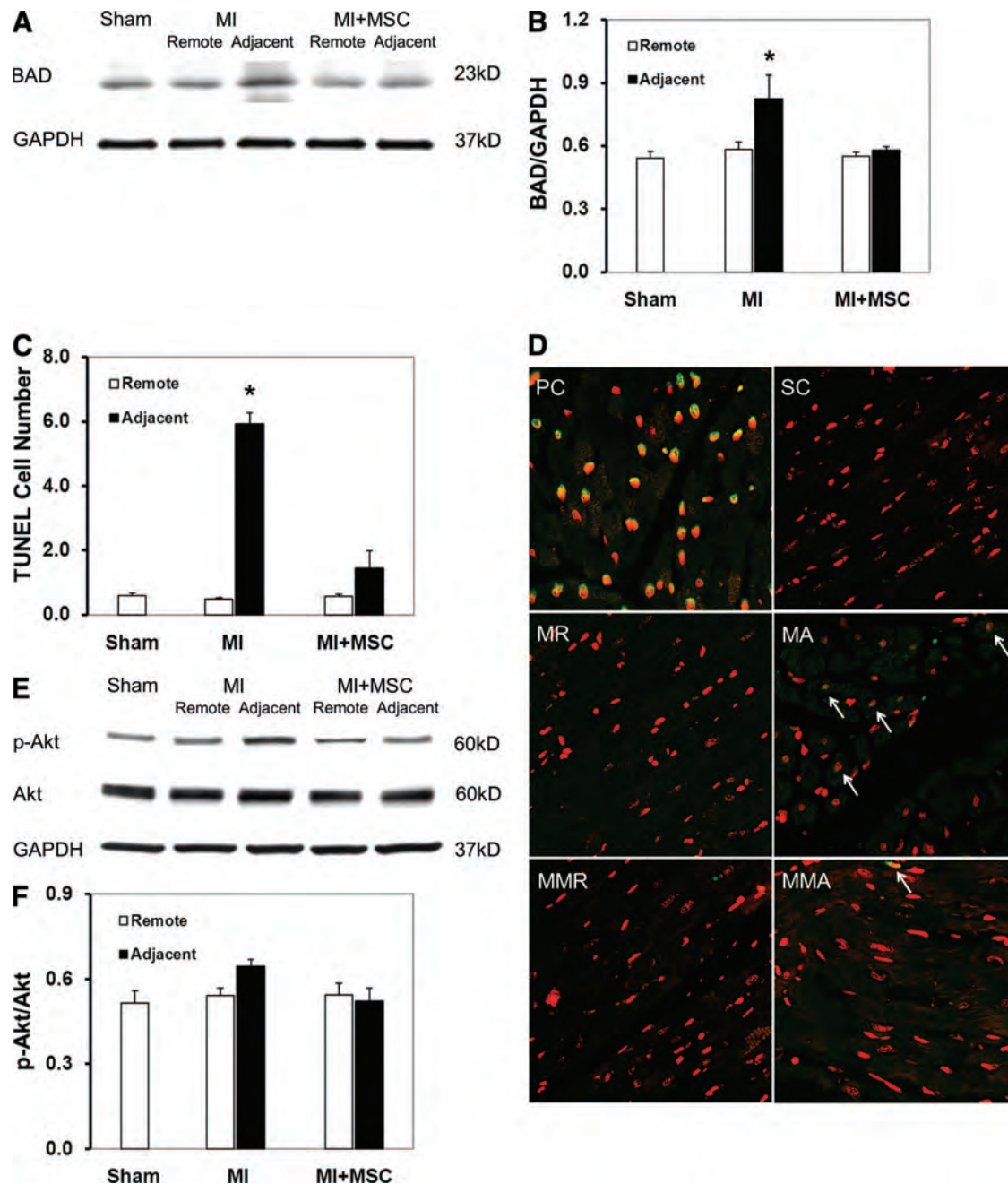


Figure 6. Normalized expression of the apoptosis-related protein Bcl-xL/Bcl-2-associated death promoter (BAD) and representative photomicrographs of in situ detection of apoptotic cells using the TUNEL assay in the adjacent and remote zones of the MI and MI+MSC groups, as well as the sham group, at 12 weeks. **(A, B):** Representative photomicrographs of Western blot, showing that the upregulation of BAD induced by myocardial infarction in the adjacent zone was normalized by MSC transplantation. **(C, D):** Representative photomicrographs ($\times 40$) of the detection of apoptotic cells using the TUNEL assay, showing the significant inhibition of apoptosis in the adjacent zone by MSC transplantation. Arrows indicate TUNEL-positive apoptotic cells in the section. The expression of Akt and p-Akt was examined in the heart regions adjacent to and remote from the infarct **(E, F)**. Although there was an increase in p-Akt in the adjacent zone of the MI animals, this either did not occur in the MI+MSC animals or was resolved by the time of sacrifice and analysis at 12 weeks. Abbreviations: GAPDH, glyceraldehyde-3-phosphate dehydrogenase; MA, adjacent zone of the MI group; MI, myocardial infarction; MMA, adjacent zone of the MI+MSC-treated group; MMR, remote zone of the MI+MSC-treated group; MR, remote zone of the MI group (no MSCs); MSC, mesenchymal stem cell; p-Akt, phospho-Akt; PC, DNase-treated positive apoptosis control; SC, sham control; TUNEL, terminal deoxynucleotidyl transferase dUTP nick-end labeling.

Alteration of cardiac strain is the reflection of the myocardium resulting from cardiac remodeling. Several aspects of cardiac remodeling, including infarct expansion, fibrosis, and cavity dilation, contribute to the alteration. Alteration of cardiac remodeling strain impairs cardiac function, resulting in further remodeling [19, 20]. Our group has previously demonstrated that

the regional remodeling strain is closely associated with the expression of proapoptotic and calcium-handling proteins, such as BAD and SERCA2a, in the adjacent zone [21, 22, 23], indicating the induction of cardiac strain alteration on cardiac apoptosis and hypertrophy. Our current results demonstrate that the remodeling strain alteration in the adjacent zone was improved by MSC

transplantation (Fig. 2D). Furthermore, the contractile strain, which reflects cardiac function, was also improved (Fig. 2B).

A hallmark response of cardiomyocytes to stress is the development of hypertrophy. Generally, cardiomyocyte hypertrophy is believed to have a compensatory function by diminishing wall stress following MI. Conversely, sustained cardiac hypertrophy represents one of the most common causes of cardiac failure [30]. In fact, studies have shown that pathological hypertrophy induced by MI is accompanied by the alteration of apoptosis regulators, resulting in increased sensitivity to apoptosis induction [31]. Our results demonstrated that cardiomyocyte hypertrophy could be significantly attenuated by MSC transplantation in the adjacent zone in large animals. Moreover, our study further demonstrated that the elevated activity of hypertrophy-related signal as evidenced by the increased expression of PI3K α , PI3K γ , and p-ERK (Fig. 4A–4E), which may lead to cardiomyocyte hypertrophy, was normalized in the adjacent zone by MSC transplantation. These results showed that MSCs could prevent regional hypertrophy induced by MI.

To date, no other study has examined the effects of MSC transplantation on the expression of the main calcium-handling proteins, SERCA2a, PLB, and NCX-1. Contractility and relaxation are mainly dependent upon the rise and fall of cytosolic Ca²⁺, closely linked to the expression/function of these Ca²⁺-regulatory proteins. Reduced function of the sarcoplasmic reticulum and accumulation of free calcium may reflect a major defect in excitation contraction coupling in human heart failure [32, 33]. Proper function of the SERCA2a pump by PLB is necessary to maintain dynamic regulation of cardiac contractility in normal conditions and during pathophysiological states [34]. The changes in intracellular calcium handling, concomitant with structural remodeling over time, could have a crucial role in progression and the hypertrophic response toward heart failure. Our results showed that the imbalance of calcium-handling proteins induced by MI was normalized by MSC delivery as evidenced by the normalization of SERCA2a, PLB, and NCX-1 in the adjacent zone. More strikingly, the activity of SERCA2a and uptake of calcium into sarcoplasmic reticulum was significantly improved by MSC transplantation, indicative of the possible mechanism of functional improvement. This may be one of the reasons that MSC transplantation can improve cardiac function after infarction.

Inhibition of cardiac apoptosis in the adjacent zone by MSC transplantation was also demonstrated at 12 weeks (Fig. 6). Cardiomyocyte apoptosis has been shown to be a key factor in the development and progression of post-MI remodeling that can lead to chronic heart failure [34]. Furthermore, we demonstrated that the activation of BAD was normalized in the adjacent zone by MSC transplantation. The ratio of phospho-Akt to total Akt was elevated in the adjacent zone of the MI animals. This elevated expression of phospho-Akt was not seen in the MI animals treated with MSC injection (Fig. 6E, 6F). It is possible that there was an earlier phospho-Akt elevation in the MSC-treated animals that was returned to normal by the time of sacrifice.

Our current studies, together with previous work performed in the pig model [10], provide direct measurable evidence of MSC inhibition of cardiomyocyte apoptosis in large animal models following infarction. These effects may be more important than the actual replacement of injured cardiomyocytes by the

implanted MSCs, which were not provided in large enough numbers to replace the damaged cells. Most investigators report that less than 1% of cells can be identified by 4 days after injection and that there is an absence of cells by 3 weeks [35–37]. In spite of their initial intuition, investigators have shown that direct transdifferentiation of MSCs into cardiomyocytes or fusion with cardiomyocytes to replace or repair heart muscle, respectively, seems to be a quantitatively insignificant part of the limited process of repair. It appears that MSCs alter the tissue microenvironment by elaboration of soluble factors that encourage angiogenesis, survival, and immune regulation, which limits inflammation. Expression of these and other yet unidentified factors may explain MSCs' capacity to promote survival and proliferation of endogenous cells [38–40], including angiogenesis, inhibition of inflammation, and apoptosis. Many of these regulatory proteins are expressed by a specific subpopulation of cells. Thus, it is likely that the functional complexity of the broad family of MSCs explains their expanded potential for therapeutic efficacy. Consistent with the paracrine theory of MSC repair, our results have indicated that injection of MSCs into the border zone of the infarct reduced the regional endothelial cell abnormalities and inhibited myocardial apoptosis.

CONCLUSION

Our study demonstrated that the maladaptive cardiac remodeling in the region adjacent to the infarct could be significantly improved by MSC transplantation, as evidenced by normalization of cardiomyocyte hypertrophy, cardiac apoptosis, calcium-handling protein expression/activity, and cardiac strain. These findings support the therapeutic effects of MSC transplantation on cardiac remodeling after myocardial infarction.

ACKNOWLEDGMENTS

This work was supported by the National Institutes of Health (Grant R01-HL081106 to B.P.G.) and the William G. McGowan Charitable Fund. G.B. is currently affiliated with the Department of Adult Cardiac Surgery, Heart Hospital G. Monasterio Foundation, Massa, Italy.

AUTHOR CONTRIBUTIONS

Y.Z.: conception and design, collection and/or assembly of data, data analysis and interpretation, manuscript writing; T.L.: conception and design, collection and/or assembly of data, data analysis and interpretation; X.W., G.B., J.H., and P.G.S.: collection and/or assembly of data; K.X.: design and performance of SERCA2a assay and ⁴⁵Ca uptake, data analysis and interpretation, manuscript writing; P.Z.: data analysis and interpretation; M.F.P.: conception and design, data analysis and interpretation, manuscript writing, final approval of the manuscript; Z.J.W. and B.P.G.: conception and design, securing financial support, data analysis and interpretation, manuscript writing, final approval of the manuscript.

DISCLOSURE OF POTENTIAL CONFLICTS OF INTEREST

The authors indicate no potential conflicts of interest.

REFERENCES

- 1 Roe MT, Messenger JC, Weintraub WS et al. Treatments, trends, and outcomes of acute myocardial infarction and percutaneous coronary intervention. *J Am Coll Cardiol* 2010;56:255–262.
- 2 González A, Ravassa S, Beaumont Jet al. New targets to treat the structural remodeling of the myocardium. *J Am Coll Cardiol* 2011;58:1833–1843.
- 3 Orlic D, Hill JM, Arai AE. Stem Cells for myocardial regeneration. *Circ Res* 2002;91:1092–1102.
- 4 Pittenger MF, Martin BJ. Mesenchymal stem cells and their potential as cardiac therapeutics. *Circ Res* 2004;95:9–20.
- 5 Hare JM. Bone marrow therapy for myocardial infarction. *JAMA* 2011;306:2156–2157.
- 6 Gnechi M, Zhang Z, Ni A et al. Paracrine mechanisms in adult stem cell signaling and therapy. *Circ Res* 2008;103:1204–1219.
- 7 Tang J, Xie Q, Pan G et al. Mesenchymal stem cells participate in angiogenesis and improve heart function in rat model of myocardial ischemia with reperfusion. *Eur J Cardiothorac Surg* 2006;30:353–361.
- 8 Toma C, Pittenger MF, Cahill KS et al. Human mesenchymal stem cells differentiate to a cardiomyocyte phenotype in the adult murine heart. *Circulation* 2002;105:93–98.
- 9 Shake JG, Gruber PJ, Baumgartner WA et al. Mesenchymal stem cell implantation in a swine myocardial infarct model: Engraftment and functional effects. *Ann Thorac Surg* 2002;73:1919–1926.
- 10 Hatzistergos KE, Quevedo H, Oskoueï BN et al. Bone marrow mesenchymal stem cells stimulate cardiac stem cell proliferation and differentiation. *Circ Res* 2010;107:913–922.
- 11 Jameel MN, Li Q, Mansoor A et al. Long-term functional improvement and gene expression changes after bone marrow-derived multipotent progenitor cell transplantation in myocardial infarction. *Am J Physiol Heart Circ Physiol* 2010;298:H1348–H1356.
- 12 Wollert KC, Meyer GP, Lotz J et al. Intracoronary autologous bone-marrow cell transfer after myocardial infarction: The BOOST randomized controlled clinical trial. *Lancet* 2004;364:141–148.
- 13 Strauer BE, Brehm M, Zeus T et al. Repair of infarcted myocardium by autologous intracoronary mononuclear bone marrow cell transplantation in humans. *Circulation* 2002;106:1913–1918.
- 14 Williams AR, Trachtenberg B, Velazquez DL et al. Intramyocardial stem cell injection in patients with ischemic cardiomyopathy: Functional recovery and reverse remodeling. *Circ Res* 2011;108:792–796.
- 15 Berry MF, Engler AJ, Woo YJ et al. Mesenchymal stem cell injection after myocardial infarction improves myocardial compliance. *Am J Physiol Heart Circ Physiol* 2006;290:H2196–H2203.
- 16 Uemura R, Xu M, Ahmad N et al. Bone marrow stem cells prevent left ventricular remodeling of ischemic heart through paracrine signaling. *Circ Res* 2006;98:1414–1421.
- 17 Schuleri KH, Feigenbaum GS, Marco Centola M et al. Autologous mesenchymal stem cells produce reverse remodeling in chronic ischemic cardiomyopathy. *Eur Heart J* 2009;30:2722–2732.
- 18 French BA, Kramer CM. Mechanisms of post-infarct left ventricular remodeling. *Drug Discov Today Dis Mech* 2007;4:185–196.
- 19 Baltabaeva A, Marciniak M, Bijmens B et al. Regional left ventricular deformation and geometry analysis provides insights in myocardial remodeling in mild to moderate hypertension. *Eur J Echocardiogr* 2008;9:501–508.
- 20 Moustakidis P, Maniar HS, Cupps BP et al. Altered left ventricular geometry changes the border zone temporal distribution of stress in an experimental model of left ventricular aneurysm: A finite element model study. *Circulation* 2002;106:1168–1175.
- 21 Kilic A, Li T, Nolan TD et al. Strain-related regional alterations of calcium-handling proteins in myocardial remodeling. *J Thorac Cardiovasc Surg* 2006;132:900–908.
- 22 Yankey GK, Li T, Kilic A et al. Regional remodeling strain and its association with myocardial apoptosis after myocardial infarction in an ovine model. *J Thorac Cardiovasc Surg* 2008;135:991–998.
- 23 Li T, Kilic A, Wei X et al. Regional imbalanced activation of the calcineurin/BAD apoptotic pathway and the PI3K/Akt survival pathway after myocardial infarction. *Int J Cardiol* 2011 [Epub ahead of print].
- 24 Migrino RQ, Zhu X, Morker M et al. Myocardial dysfunction in the periinfarct and remote regions following anterior infarction in rats quantified by 2D radial strain echocardiography: An observational cohort study. *Cardiovascular Ultrasound* 2008;6:17–25.
- 25 Ratcliffe MB. Non-ischemic infarct extension: A new type of infarct enlargement and a potential therapeutic target. *J Am Coll Cardiol* 2002;40:1168–1171.
- 26 Kyte J. Purification of the sodium- and potassium-dependent adenosine triphosphatase from canine renal medulla. *J Biol Chem* 1971;246:4157–4165.
- 27 Xu KY, Zweier JL, Becker LC. Hydroxyl radical inhibits sarcoplasmic reticulum Ca²⁺-ATPase function by direct attack on the ATP binding site. *Circ Res* 1997;80:76–81.
- 28 Chu A, Dixon MC, Saito A et al. Isolation of sarcoplasmic reticulum fractions referable to longitudinal tubules and junctional terminal cisternae from rabbit skeletal muscle. *Methods Enzymol* 1988;157:36–46.
- 29 Xu KY, Zweier JL, Becker LC. Functional coupling between glycolysis and sarcoplasmic reticulum Ca²⁺ transport. *Circ Res* 1995;77:88–97.
- 30 Xu D, Li N, He Y et al. Prevention and reversal of cardiac hypertrophy by soluble epoxide hydrolase inhibitors. *Proc Natl Acad Sci USA* 2006;103:18733–18738.
- 31 Kang PM, Yue P, Liu Z et al. Alterations in apoptosis regulatory factors during hypertrophy and heart failure. *Am J Physiol Heart Circ Physiol* 2004;287:H72–H80.
- 32 Houser SR, Piacentino V III, Weisser J. Abnormalities of calcium cycling in the hypertrophied and failing heart. *J Mol Cell Cardiol* 2000;32:1595–1607.
- 33 Houser SR, Margulies K. Is depressed myocyte contractility centrally involved in heart failure? *Circ Res* 2003;92:350–358.
- 34 Periasamy M, Bhupathy P, Babu GJ. Regulation of sarcoplasmic reticulum Ca²⁺ ATPase pump expression and its relevance to cardiac muscle physiology and pathology. *Cardiovasc Res* 2008;77:265–273.
- 35 Kajstura J, Rota M, Whang B et al. Bone marrow cells differentiate in cardiac cell lineages after infarction independently of cell fusion. *Circ Res* 2005;96:127–137.
- 36 Noiseux N, Gnechi M, Lopez-Llascas M et al. Mesenchymal stem cells overexpressing Akt dramatically repair infarcted myocardium and improve cardiac function despite infrequent cellular fusion or differentiation. *Mol Ther* 2006;14:840–850.
- 37 Zhang S, Wang D, Estrov Z et al. Both cell fusion and transdifferentiation account for the transformation of human peripheral blood CD34-positive cells in cardiomyocytes in vivo. *Circulation* 2004;110:3803–3807.
- 38 Lee R, Seo MJ, Reger RL et al. Multipotent stromal cells from human marrow home to and promote repair of pancreatic islets and renal glomeruli in diabetic pancreatic islets and renal glomeruli in diabetic NOD/scid mice. *Proc Natl Acad Sci USA* 2006;103:17438–17443.
- 39 Mahmood A, Lu D, Chopp M. Marrow stromal cell transplantation after traumatic brain injury promotes cellular proliferation within the brain. *Neurosurgery* 2004;55:1185–1193.
- 40 Munoz J, Stoutenger BR, Robinson AP et al. Human stem/progenitor cells from bone marrow promote neurogenesis of endogenous neural stem cells in the hippocampus of mice. *Proc Natl Acad Sci USA* 2005;102:18171–18176.